Songklanakarin J. Sci. Technol.
30 (6), 755-760, Nov. - Dec. 2008

Songklanakarin Journal of Science and Technology
http://rdo.psu.ac.th/sjst

Original Article

Determination of optimum rotational speed of heterogeneous catalytic reactor using computational fluid dynamic

Rungrote Kokoo[1]*, Phavanee Narataruksa[2], Karn Pana-Suppamassadu[2] and Sabaithip Tungkamani[3]

[1] *The Sirindhorn International Thai-German Graduate School of Engineering,*

[2] *Department of Chemical Engineering, Faculty of Engineering,*

[3] *Department of Industrial Chemistry, Faculty of Apply Science,*
King Mongkut's University of Technology North Bangkok, Bang Sue, Bangkok, 10800 Thailand.

Received 22 January 2008; Accepted 19 September 2008

Abstract

Solid suspension in a stirrer tank reactor is relevant in many chemical process industries. For a heterogeneous catalytic reactor, the degree of solid suspension is a crucial parameter in the design and scaling-up processes. The suspension of solid catalysts at a minimum impeller speed can reduce the operating cost of processes. To ensure optimum conditions for suspension, a 3D simulation technique by Computational Fluid Dynamic (CFD) was used to study flow characteristics in a heterogeneous catalytic reactor. A case study of a 200 milliliter cylindrical reactor was modeled together with equipped parts, i.e. a sampling port, 2 baffles, one thermocouple and a mechanical stirrer. The results show that the total velocity increases from the impeller's center to the impeller's tip and decreases from the impeller's tip to the side wall of the reactor. The vertical velocity at the bottom of the impellers directs flow upward while the velocity at the top directs flow downward. These simulations provide a good preview of solid suspension without doing experiments. It is recommended that the vertical velocity at the bottom of the reactor is in the range between minimum fluidization velocity and terminal velocity to ensure solid suspension in the system.

Keywords: solid suspension, heterogeneous catalytic reactor, computational fluid dynamic

1. Introduction

Solid suspension in a stirrer tank reactor is relevant in many process industries such as mineral processing, crystallization, biochemical processes. A catalyst may be present in solid phase in chemical reactors such as the reactors for catalytic hydrogenation, Fischer-Tropsch synthesis and the production of polymers (Murthy, 2007). In a heterogeneous catalytic reactor, the solid suspension performance is a crucial parameter. The suspension of solid catalyst at a minimum impeller speed can reduce power consumption that influence in the process economics (Dohi, 2004).

The influence of hydrodynamic mixing on solid suspension in reactors were investigated by experiments at various configurations and parameters such as: single impeller, multi impeller, various impeller clearances, various impeller types, varying fluid viscosity and varying solid loading to find the minimum impeller speed and minimum power consumption (Zwietering, 1958; Nienow, 1996; Murugesan, 2001; Montante *et al.*, 2003; Pinelli and Magelli, 2001). The critical impeller speed (N_{js}) was defined by Zwietering (1958) to avoid deposition of solid on the bottom of the reactor.

$$N_{js} = S \frac{d_p^{0.2} \nu^{0.1} (g(\rho_p - \rho_f))^{0.45} \phi^{0.13}}{\rho_f^{0.45} D^{0.85}} \quad (1)$$

*Corresponding author.
Email address: kim_kokoo@hotmail.com

However, the Zwietering equation was found unsuitable for prediction of N_{js} at high fluid viscosity (Nienow, 1999) and the experimental results can be applied only to systems under study (Kee and Tan, 2002; Montante *et al.*, 2003). Different flow behaviors result from each reactor variation including variations in reactor geometry, variations in fluid properties, variations in catalyst properties, variations in impeller types and variations in reactor equipment (baffle, sampling tube and thermowell).

Simulation techniques using CFD can be used to obtain possible flow patterns and the magnitude of the fluid velocity within the reactor (Montante *et al.*, 2001). Three-dimensional analysis is necessary for the study of fluid flow direction in an unsymmetrical reactor (Oching and Lewis, 2004). However, previous works focused on the average total fluid velocity of the entire reactor (Graf, 1971), on the total fluid velocity at the bottom of reactor (Lee, 2002) rather than the vertical fluid velocities near the bottom which are important for solid suspension in terms of upward lifting force.

Due to the increase in oil prices and environmental concerns, biodiesel has become a substitute for petroleum diesel. The production of biodiesel using heterogeneous catalytic reactors is an alternative to overcome the high separation cost of homogeneous processes. A factor of particular importance to the transesterification process is the degree of mixing between the immiscible fluid (methanol and vegetable oils) and suspending solid particles (catalyst). Mechanical mixing is normally applied to increase the contact time between the reactants, resulting in an increase in mass transfer and reaction rates (Gerpen *et al.*, 2004 and Noureddini *et al.*, 1997).

In the present work, the fluid velocity profile in a heterogeneous catalytic reactor for biodiesel production was investigated using the computational fluid dynamic technique. The objective was to find the optimum rotational speed for mixing in order to keep the magnitude of velocity at the bottom of the reactor higher than the minimum fluidization velocity. In that case, suspension of solid particle can occur in the reactor.

2. Dynamic of Particle

The fluid motion on the particle surface is evaluated from a balance of the upward lifting force (F_U) and downward force (F_D). At the initial movement, the particle was assumed as no cohesiveness and looseness. Particle settling as show in Figure 1 is governed by two forces that can be expressed as:

$$F_U = \frac{C_D \rho_f A_P U_t^2}{2} \quad (2)$$

Where C_D is the drag coefficient, A_p is the particle's projected area and U_t is the terminal velocity.

$$F_D = gV_P(\rho_p - \rho_f) \quad (3)$$

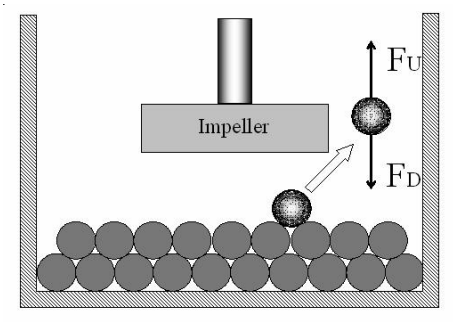

Figure 1. Bottom of the heterogeneous catalytic reactor

Where V_P is the particle's volume, g is the gravitational force, ρ_p is the particle density and ρ_f is the fluid density. At the point that the particle would just begin to rise, the upward force equals the downward force, so that equation (2) equals equation (3). The terminal velocity can be express as:

$$U_t = \left[\frac{4d_P(\rho_P - \rho_f)g}{3\rho_f C_D}\right]^{0.5} \quad (4)$$

For spherical particles (Daizo, 1990), the drag coefficient can be expressed as:

$$C_D = \frac{24}{\mathrm{Re}_P} + 3.3643\,\mathrm{Re}_P^{0.3471} + \frac{0.4607\,\mathrm{Re}_P}{\mathrm{Re}_P + 2682.5} \quad (5)$$

Where Re_P is the particle Reynolds number. Equation 2 to equation 5 will be employed for determining the operation conditions of the reactor.

For spherical particles, the dimensionless particle diameter d_P^* can be defined as:

$$d_P^* = d_P\left[\frac{\rho_f(\rho_P - \rho_f)g}{\mu^2}\right]^{0.333} \quad (6)$$

The ratio between U_t and minimum fluidization (U_{mf}) strongly depends on particle size (Daizo and Octave, 1990) and can be expressed as:

For fine solid particle, i.e., $d_P^* < 1$: $\frac{U_t}{U_{mf}} = 78$ (7)

For large solid particle, $d_P^* > 100$: $\frac{U_t}{U_{mf}} = 9.2$ (8)

3. Simulation Procedure

The cylindrical reactor's height and diameter are 9.0 cm and 5.5 cm respectively, with two baffles of width 0.6 cm and of height 8.0 cm, a sampling tube of diameter 0.6 cm and a thermocouple of diameter 0.3 cm. The multiple impellers are set-up as shown in Figure 2a. The continuous phase is palm oil which has a density and viscosity of 908 kg/m^3 and 28.65 mm^2/s respectively (Jitputti *et al.*, 2006).

The radial velocity (V_r) of the liquid at the blade tips

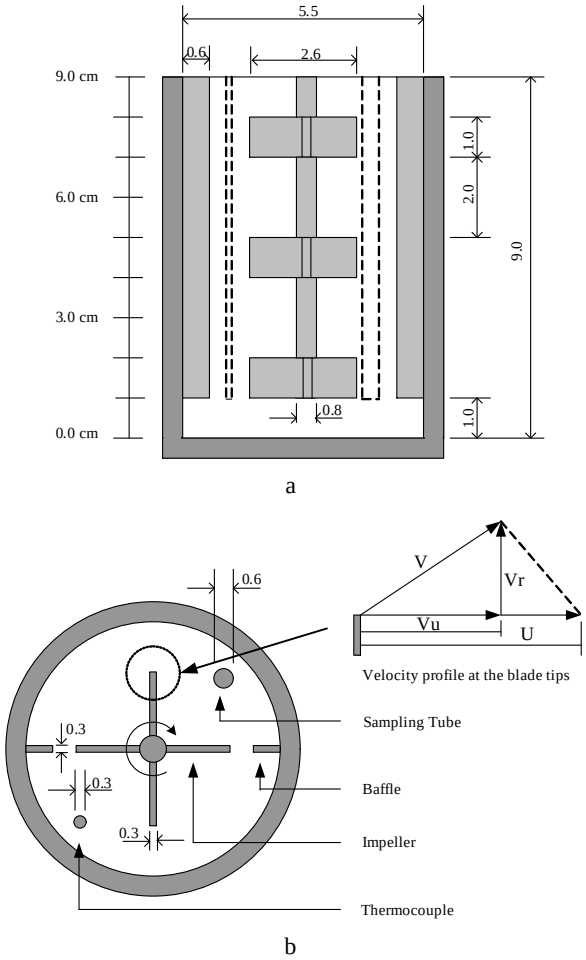

Figure 2. Reactor; a = Front view, b = Top view

is approximately 0.6 times the tip speed velocity (U). The total velocity (V) at the same point is slightly less than the tip speed, i.e. 0.95 U. The tangential velocity (V_u) of the liquid at the blade tips can be calculated from the velocity profile of the blade tips as show in Figure 2b and is equal to 0.736U (McCabe, 2001).

The tip speed velocity is a function of the impeller radius and can be calculated from equation 6 (McCabe, 2001).

$$U = \frac{rpm \times \pi \times r}{30} \quad (9)$$

Where r is the radius of the impeller.

In this study; the flow pattern in the reactor was obtained by using COMSOL MULTIPHYSICS program version 3.3. Characteristics of fluid flow in the reactor were investigated via velocity profiles. Calculations of flow properties in a batch reactor are based on mathematical models for the conservation of momentum and mass by use of the Incompressible Navier-Stokes Equations.

$$\rho \frac{D}{Dt}\vec{v} = -\nabla p + \mu \nabla^2 \vec{v} + \rho g \quad (10)$$

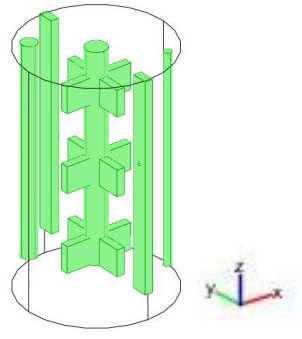

Figure 3. Simulation geometry of reactor

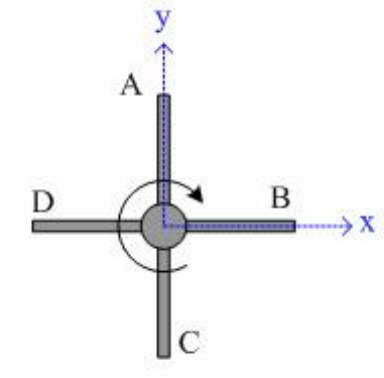

Figure 4. Impeller's top view

A 3D application mode is used to model the entire reactor. The reactor is equipped with a sampling tube, a baffle, a thermocouple and a mechanical stirrer as show in Figure 3. The fluid velocity at the impeller as show in Figure 4 was set as following;

A and C:	0.736×U	x-velocity
	0.600×U	y-velocity
B and D:	0.600×U	x-velocity
	-0.736×U	y-velocity

At the top reactor surface, the pressure condition is set and the condition of another surface is assigned the no slip condition.

4. Results and Discussions

Figure 5 represents the simulation results showing the total fluid velocity profile inside the reactor at 100 rpm and 200 rpm. The results show that the total fluid velocity increases from the impeller's center to the impeller's tip and decreases from the impeller's tip to the side wall of the reactor for all impellers in accordance with the theory of agitation and mixing of liquid (McCabe, 2001).

The illustrations of arrow velocity and streamline

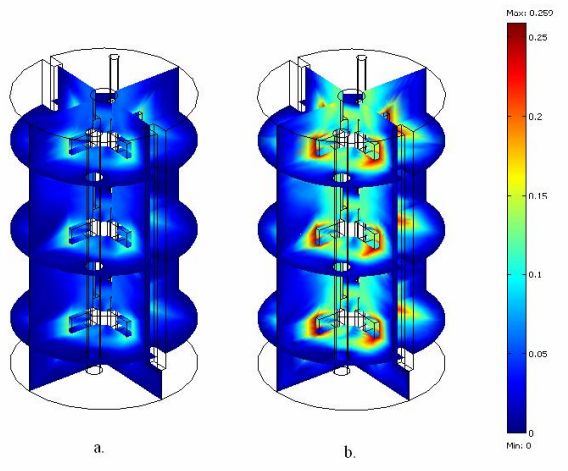

Figure 5. Total fluid velocity; a = 100 rpm, b = 200 rpm

velocity are shown in Figure 6. This confirms the clockwise direction of fluid flow.

Cross-sectional slices of the velocity profile in the z direction at 100 rpm, 150 rpm 200 rpm and 250 rpm are shown in Figure 7. Where red indicates upward velocity and blue indicates downward velocity. From the figure, increasing of the velocity in z direction (upward velocity and downward velocity) is found to be proportional to the rotational speed. The upward velocity component is critical to ensuring suspension of the solid phase.

Fluid velocity (z direction) at the bottom of the impeller is directed upward from the impeller's center to the impeller's tip and is directed downward from the impeller's tip to side wall of the reactor.

The fluid velocity (z direction) at the top of the impeller is directed downward from the impeller's center to the impeller's tip and is directed upward from the impeller's tip to side wall of the reactor as a result of the system geometry.

The fluid velocity (z direction) profile at the bottom (z = 0.001 m) of the reactor is shown in Figure 8. The highest fluid velocity (flow upward) is at the impeller. It is found

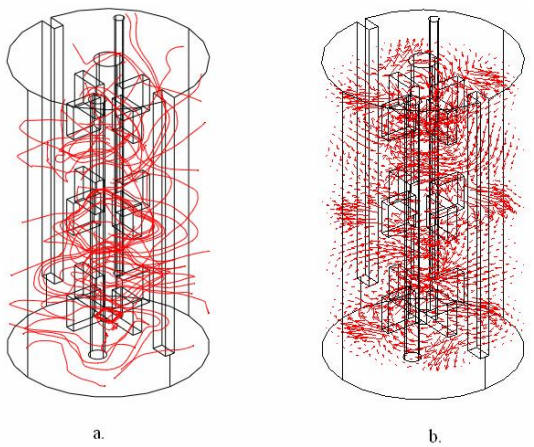

Figure 6. a = streamline velocity, b = arrow velocity at 200 rpm

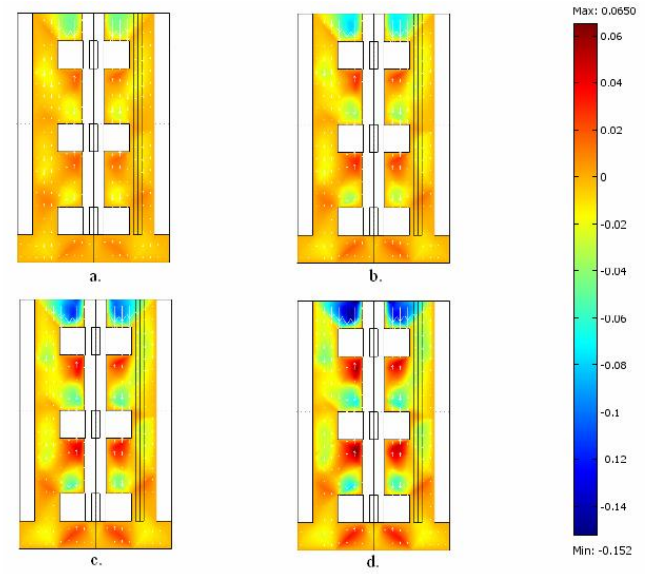

Figure 7. Fluid velocity (z direction) at different rotational speeds; a = 100 rpm, b = 150 rpm, c = 200 rpm and d = 250 rpm

that fluid velocity increases when rotational speed increases.

The important factors in a heterogeneous catalytic reactor are the particle properties (size and density) and the fluid properties (viscosity and density). Therefore, the terminal velocity and the minimum fluidization velocity strongly depend on the catalyst size as shown in Figure 9.

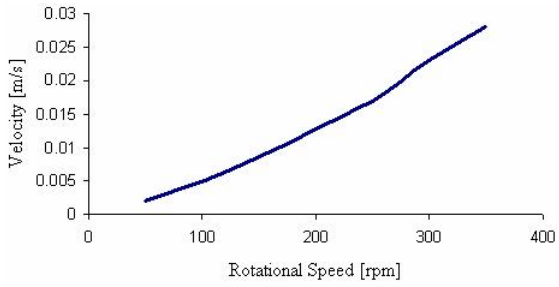

Figure 8. Velocity (z direction, z = 0.001m) at different rotational speeds

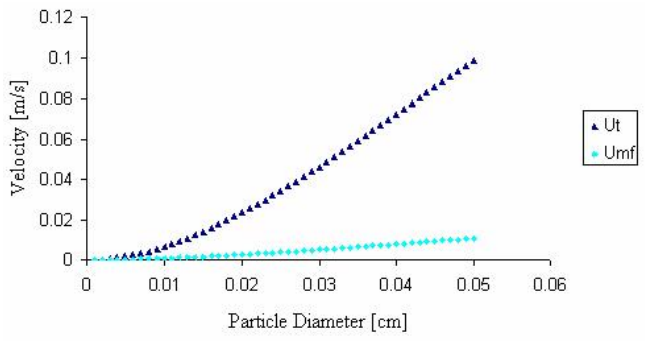

Figure 9. Terminal velocity and minimum fluidization velocity of catalyst

The results appeared in Figure 9 were obtained by applying equation 4 to equation 8 to solid particle of size less than 0.0065 cm in diameter.

A plot between the particle diameter and the rotational speed shown in Figure 10 represents the rotational speed that is suitable for biodiesel production using a solid catalyst at solid density 4.2 g/cm^3. Figure 10 is obtained by integrating the results of Figure 8 and Figure 9. With Figure 10, the suitable rotational speed can be obtained when the particle diameter is specified, for example, for the particle diameter of 0.002 cm, the suitable rotational speed is 200 rpm.

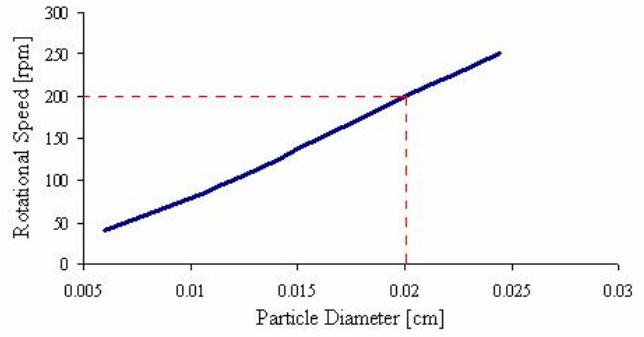

Figure 10. Rotational speed vs. particle diameter

5. Conclusions

The optimum rotational speed for mixing in a heterogeneous catalyst reactor is simulated by computational fluid dynamic to optimize suspension of solid particles in the reactor. The modeling results will help determine the suitable rotational speed that is a function of particle's size and particle's density. To ensure suspension of the particle, fluid velocity (z direction) at the bottom of the reactor is kept between minimum fluidization velocity and terminal velocity.

Nomenclature

A_P	particle's projected area
C_D	drag coefficient
d_p	particle diameter
d_P^*	dimensionless particle diameter
g	gravitational force
D	impeller diameter
F_U	upward lifting force
F_D	downward force
N_{js}	critical impeller speed
Re_P	particle Reynolds number
r	radius of the impeller
S	geometry dependent coefficient
U	tip speed velocity
U_{mf}	minimum fluidization velocity
U_t	terminal velocity
V	total fluid velocity
V_P	particle's volume
V_r	radial velocity of the liquid leaving at the blade tips
V_u	tangential velocity of the liquid leaving at the blade tips
ρ_f	fluid density
ρ_P	particle density
ϕ	initial solid mass fraction
ν	kinematic viscosity of fluid

Acknowledgments

This work was supported by The Sirindhron International Thai-German Graduate School of Engineering (TGGS). The authors wish to thank the Department of Chemical Engineering for simulation software and the Department of Industrial Chemistry for catalyst properties and thesis funds.

References

Daizo K. and Octave L. 1990. Fluidization Engineering 2nd, Butterworth-Heinemann, Boston, USA., pp. 80-83.

Dohi, N., Takahashi, T., Minekawa, K., and Kawase, Y. 2004. Power consumption and solid suspension performance of large-scale impellers in gas–liquid–solid three-phase stirred tank reactors. Chemical Engineering. 97, 103-114.

Gerpen, J. Van., Shanks, B., and Pruszko, R. 2004. Biodiesel Production Technology, National Renewable Energy Laboratory.

Graf, W.H. 1971. Hydraulics of Sediment Transport, Mc Graw-Hill, New York, U.S.A.

Jitputti, J., Kitiyanan, B., Rangsunvigit, P., Bunyakiat, K., Attanatho, L., and Jenvanitpanjakul, P. 2006. Transesterification of crude palm kernel oil and crude coconut oil by different solid catalysts. Chemical Engineering. 116, 61-66.

Kee, C.S., and Tan, B.H.R. 2002. CFD simulation of solids suspension in mixing vessels. Chemical Engineering of Canadian. 80, 1-6.

Lee, S.Y. 2002. Agitator Mixing Analysis in a HB-Line Flat Tank. U.S. Department of Energy.

McCabe, L. Warren. 2001. Unit Operation of Chemical Engineering, McGraw-Hill, Singapore., pp. 239-258.

Montante, G., Micale, G., Magelli, F. and Brucanto, A. 2001. Experimental and CFD prediction of solid particle distribution in vessel agitated with four pitched blade turbines. Transactions of Chemical Engineering. 79A, 1005-1010.

Montante, G., Pinelli, D., and Magelli, F. 2003. Scale-up criteria for the solid distribution in slurry reactors stirred with multiple impellers. Chemical Engineering Science., 58, 5363-5372.

Murthy, B.N., Ghadge, R.S., and Joshi, J.B. 2007. CFD simulations of gas–liquid–solid stirred reactor: Prediction

of critical impeller speed for solid suspension. Chemical Engineering Science., 62, 7184-7195.

Murugesan, T. 2001. Critical impeller speed for solids suspension in mechanically agitated contactors. Chemical Engineering of Japan., 34, 423-429.

Nienow, A.W. 1996. Mixing studies: a comparison of Rushton turbine with some modern impellers. Chemical Engineering Research and Design 74(A1).

Nienow, A.W. and Lbrahim S. 1999. Comparing Impeller Performance for Solid-Suspension in the Transitional Flow Regime with Newtonian Fluids. Chemical Engineering Research and Design., 77, 721-727.

Noureddini, H. and Zhu, H. 1997. Kinetic of transesterification of soybean oil. Journal of American Oil Chemists' Society, 74, 1457-1463.

Ochieng, A., and Lewis, A.E. 2004. CFD simulation of mixing and power consumption in a tank with a low impeller clearance. Proceedings of South African Conference on Applied Mechanics., 81,1-9.

Pinelli, D., and Magelli, F. 2001. Solid distribution in slurry reactors with dilute pseudoplastic suspensions. Industrial and Engineering Chemistry Research., 40, 4456-4462.

Zwietering, T.N.H. 1958. Suspending of solids particle in liquid by agitators. Chemical Engineering Science., 8, 244-253.